FORMATION OF ADIABATIC SHEAR BANDS IN ORTHOGONAL MACHINING OF TI6AL4V ALLOY

O. Friderikos[1], A. Korlos[2], C. David[3], D. Sagris[3] and G. Mansour[4]

[1]LMT-Cachan, ENS Cachan/CNRS/PRES UniverSud Paris
61 avenue du president Wilson, Cachan, F-94230, France
email: friderikos@lmt.ens-cachan.fr

[2]Department of Vehicle Technology, Laboratory for Machine Tools and Manufacturing Processes
Faculty of Technological Applications, Technological Educational Institute of Thessaloniki
Thessaloniki, GR-57400, Greece
e-mail: apkorlos@vt.teithe.gr

[3]Mechanical Engineering Department, Laboratory of Manufacturing Technology & Machine Tools
Faculty of Applied Technologies, Technological Education Institute of Central Macedonia
Serres, GR-62124, Greece
e-mail: david@teiser.gr, e-mail: dsagris@teiser.gr

[4]Mechanical Engineering Department, Laboratory for Machine Tools and Manufacturing Engineering
Aristotle University of Thessaloniki
Thessaloniki, GR-54124, Greece
e-mail: mansour@eng.auth.gr

Keywords: Adiabatic Shear Bands, FEM, Orthogonal machining.

Abstract.*A systematic study has been undertaken to examine the mechanism of Adiabatic Shear Band (ASB) formation in orthogonal machining of Ti6Al4V alloy. First a critical review is given of the currently theoretical models in order to delineate the salient features of the assumed mechanisms of ASB. Among them, thermally aided shear instability and/or fracture mechanics have been proposed to explain the destabilization of the homogeneous plastic deformation which gives rise to localized, band-like adiabatic shear deformation. The purpose of this review is to bring out the fact that the various theoretical concepts or approaches involve some degree of uncertainty about the mechanisms and the role played by the influencing factors. From a modeling point of view a coupled thermomechanical rigid viscoplastic finite element model is applied to predict the ASB in large strain, high strain rate and temperature. Fracture criteria are also implemented to obtain a deeper understanding of the material damage with growth of voids and/or micro-cracks inside the adiabatic shear zone.*

1 INTRODUCTION

Ti6Al4V alloy is widely used in aerospace, chemical, automotive and biomedical industry due to its unique strength to weight ratio and its exceptional resistance to corrosion. However, a major problem in machining of Ti6Al4V is the rapid tool wear when the cutting velocity range is set beyond 60 m/min. Therefore, Ti6Al4V is characterized by poor machinability due to low material removal rates and short cutting tool life. The reason of this behavior can be traced back to the mechanisms that take place during chip formation. Significant effort has been placed in the past to explain the segmented chip formation but the mechanism is still not well understood. Different theoretical foundations are proposed to explain the catastrophic shear instability. To this end, thermally-aided shear instability was first proposed by Zener and Hollomon using the term 'Adiabatic Shear Band' (ASB) [1]. They observed a shear band during punching of a hole in a low carbon steel plate. They stated that, at the onset of the shear band, the material becomes unstable when thermal softening becomes greater than the strain hardening. Moreover, Recht postulated that catastrophic shear occurs when the rate of change of the flow stress with plastic strain equals zero, and therefore a negative slope implies an intrinsic instability of the material [2].

When certain conditions are met, plastic deformation under high strain rates is accompanied with the formation of adiabatic shear bands. If thermal softening outweighs strain and strain rate hardening, it may eventually destabilize the homogeneous plastic deformation and give rise to localized, band-like adiabatic shear deformation. These narrow zones of very large shear strain initiate and propagate in a previously homogeneous deformed region. The material inside the band preserves its integrability (no cracks occur inside the band). The

width of adiabatic shear bands may be of the micron range (10-100μm), whereas the lateral extend may be hundreds or even thousands of times bigger. In titanium alloys, adiabatic shear banding is enforced by the low value of the heat conductivity (≈16 W/mK). Adiabatic shear bands have a substantial effect in high speed deformation and significantly alter the mechanical behavior of the material in question. In many cases these are often precursors to further damage and provide initiation sites and propagation paths for cracks. A thorough overview of the underlying physics of ASB can be found in a monograph of T. W. Wright [3]. During high speed machining, adiabatic shear bands are formed intermittently in a periodic manner if certain conditions are met. Due to this destabilizing mechanism, segmented chips occur in contrast to continuous chip formation. Material damage associated with growth of voids and/or micro-cracks inside the shear zone has been proposed as an alternative mechanism of segmented chip formation [4-7]. The periodic crack formation theory has been successfully used to explain the chip formation during the machining of hard steel. According to this theory, fracture exists in all types of chip formation, even in continuous chips. Detailed information on the crack generation theory is provided by Shaw et al. [4], [8].

To better understand the dynamic material behavior of Ti6Al4V it may be well to summarize its crystalline structure. Ti6Al4V consists of two crystalline phases; a low temperature α phase (hcp) and a high temperature βphase (bcc). The hcp lattice affords a limited number of slip planes in contrast to bcc lattice in which more slip systems exist, increasing the ductility. Ti6Al4V undergoes allotropic transformation from hcp to bcc structure between 800^{o}C and 850^{o}C (βtransus temperature). Below transus temperature, the microstructure of Ti6Al4V consists of α and β grains with the fraction of β grains increasing with temperature. Komanduri explained the change of chip morphology from discontinuous at low cutting speeds to segmented but continuous at high cutting speeds due to the allotropic transformation of the α phase [9]. Furthermore, Rogers [10] has classified the ASB into 'deformed' and 'transformed' types. In the latter, a crystallographic phase change occurs due to intense deformation, heat evolution and rapid cooling, producing a phase transformation.

The present work is aimed at a comprehensive simulation of the formation and propagation of adiabatic shear bands in orthogonal machining. During the course of this analysis, at the first configuration models, fracture is clearly separated from ASB and no criterion for the nucleation and growth of voids and/or micro-cracks is considered. Therefore, the simulation of ASB is considered as a result similar to Recht's mechanism of catastrophic thermoplastic shear [2]. Additional configuration models including ductile fracture criteria are also implemented into the FEM code in order to investigate the major aspects of the physical deformation and failure processes, identifying the ASB propagation mechanism.

2 FEM MODELING OF HIGH SPEED MATERIAL PROCESSING

The thermomechanical coupling and the highly nonlinear nature of the deformation process makes difficult to obtain solutions through analytical methods. In this paper, a rigid-viscoplastic finite element formulation is applied to simulate the localization of shear instability, where the elasticity effects are completely neglected. This method has been extensively used previously for the prediction of material response during metal forming and more recently in machining processes. A thorough overview of the foundation theory and many interesting results can be found in [11], [12]. From a mechanical point of view the basic equations that have to be satisfied are the equilibrium equation, the incompressibility condition, the material constitutive relationship and the boundary conditions. Since it is extremely difficult to find a complete solution that satisfies all of the governing equations and the associated high non-linerar boundary conditions, an approximate solution is obtained in a weak form using the variational principle. After discretization of the variational functional we finally get a non-linear set of equations. The solution of the stiffness equation can be determined either by the direct iteration method and/or by the conventional Newton-Raphson iterative method.

During orthogonal machining, substantial amounts of heat are generated due to plastic deformation and friction at the tool-chip interface. The high temperatures have a considerable influence on the mechanical response of the materials in question. In the present analysis, the temperature field is determined by solving the energy balance equation, which is rewritten by using the weighted residual method. The finite element discretization procedure is then applied to solve the latter expression.

The updated Lagrangian formulation is used to describe the large deformation. However, one of the main limitations of the updated Lagrangian method for large deformation problems is the excessive element distortion, which leads to unacceptably small time steps and numerical instability of the solution. A suitable way to overcome the element distortion is to use a remeshing process. This process is triggered automatically when either a zero or a negative Jacobian is encountered in a finite element, or on assignment of certain defined criteria. When the above conditions are met, the simulation is interrupted and a new mesh is calculated conforming to the current state of the geometry using an automatic mesh generation. It has to be stated, that there is a substantial cost associated with frequent remeshing, because there is an inherent uncertainty in preserving the state variable data in the re-mapping process.

Adaptive mesh refinement is an indispensable part of finite element modeling in order to resolve steep gradients which may be present in the solution. Furthermore, leads to a considerable reduction in the number of

degrees of freedom. It provides a powerful tool for achieving high accuracy in the solution without increasing the computational resources. Weighting factors that specify the relative mesh density to regions of high curvature or of steep strain, strain rate and temperature gradients can be assigned individually [13]. Additionally, areas can also be specified geometrically to generate a fine or coarse mesh using mesh density windows. In this way, mesh adaptivity helps to maintain a high-quality mesh in the primary shear zone where the ASB initiate and propagate.

It is interesting to note that mesh generation is not a trivial problem for the numerical simulation of adiabatic shear bands, as their formation and evolution is quite sensitive to the mesh. Several approaches have been used to decrease mesh dependence for shear bands [14], [15]. Additionally, implementation of fracture criteria into the FEM code requires a high mesh refinement in the primary shear zone. It is also well known that an improved understanding of the implications of minimum length scales is needed for the convergence and efficiency of numerical computations. In order to adequately tackle this issue, a high degree of mesh refinement is required [16]. During the thermomechanical calculations of high speed machining, it is evident that the length scale of the mesh regulates the spatial evolution of the state variables. In order to resolve the physical and constitutive features of the material, the element size must be below of a threshold value. Estimation of this threshold is not an easy task as it is strongly dependent on the underlying physics of the process. Thus, for example, the size of elements in the region where an adiabatic shear band may nucleate must be smaller than its width. Otherwise, the prediction of adiabatic shear bands would be delayed or even be impossible.

3 MATERIAL FLOW STRESS AND BOUNDARY CONDITIONS

One of the critical issues in high strain-rate deformation is the reliability and accuracy of the flow stress models to represent the material behavior due to the various localized physical mechanisms involved in the process. High-speed deformation tests, such as the Split-Hopkinson-Pressure-Bar (SHPB) can only reach strains below 0.5 and strain rates in the range of 10^2-10^4 s^{-1} [17]. In machining of Ti6Al4V alloy the strains (>1) and strain rates (10^3-$10^7 s^{-1}$ or even higher) in the primary shear zone are far beyond the experimental determined range. Therefore, the mechanical behavior of Ti6Al4V has to be extrapolated over several orders of magnitude. In the present work, a flow stress equation described as a function of strain, strain rate and temperature [18] has been employed, included in the material database of DEFORM-2D. An interesting parametric study of a phenomenological material flow stress law on chip segmentation can be found in [19].

Part of the mechanical energy expended during a plastic deformation process in metals is converted into heat, while the remaining is stored in the material microstructure (cold work). The stored energy is an essential feature of the cold-worked state, and represents the change in internal energy of the metal. In addition, the stored energy of cold work remains in the material after removal of the external loads. Since thermal evolution is crucial in shear band initiation and growth, accurate knowledge of the thermomechanical conversion, also known as Taylor-Quinney coefficient β, is necessary to produce reliable finite element simulations [20]. The fraction of the plastic work being converted to heat is generally assumed to be a constant parameter of 0.9, for most metals. However, experimental tests with Ti6Al4V showed that the inelastic heat fraction coefficient can be strongly dependent on strain and strain-rate, and there are no unanimous agreements on the fraction of plastic work conversion into thermal energy during high strain rate deformation [21-24]. Thermodynamical foundations leading to the observed plastic strain and strain rate dependence of β have been discussed by Rosakis et al. [25]. Therefore, in order to accurately study the catastrophic shear mechanisms, a constitutive equation relating the coefficient β with strain and strain rate must be established.

In the temperature analysis, a thermal contact conductance of 105 $W/m^2 K$ is assigned to the contacting tool/workpiece interface. This constant is related to the thermal contact resistance across the interface of the contacting objects. Heat convection between the workpiece and air is allowed through a heat transfer coefficient of 20 $W/m^2 K$. The tool/workpiece boundary conditions are quite complex, influenced by a number of factors such as the cutting speed, feedrate, chemical composition of the tool and the workpiece, etc. [26]. While several models have been proposed to determine the friction boundary conditions, an accurate description is still unavailable and the correlation with experimental data can in general be deemed as poor. To the best of the authors' knowledge, there are conflicting viewpoints concerning the nature of the friction conditions to the point where definitive conclusions cannot be easily drawn [27]. At the present model, a shear friction law is used defined by the following relationship:

$$\tau_f = m \cdot k \tag{1}$$

$$k = \frac{\bar{\sigma}}{\sqrt{3}} \tag{2}$$

wherem ($0<m\leq1$) is the friction factor, k is the material shear yield stress and $\bar{\sigma}$ is the effective yield stress under pure uniaxial tension.

4 NUMERICAL RESULTS

4.1 Overview

In this numerical study a 2D plane strain model for the simulation of chip formation in orthogonal machining is used due to the small gradients of the state variables, (i.e. temperature, strain, strain rate, stress, etc.), in the direction parallel to the cutting edge. It is assumed that the workpiece and the cutting tool are initially at a uniform ambient temperature T_0=25 ^{o}C. The workpiece geometry is defined as a rectangular block with large enough dimensions to reduce the effects of the boundary conditions (Figure 1). The tool movement is constrained both horizontally and vertically, while the workpiece moves due to a horizontal velocity component prescribed at the left and the bottom boundary nodes. A constraint to vertical direction is additionally applied to the left and the bottom boundary workpiece nodes. A minimum element size of about 0.4-1.6 μm is generated in the region of intense shearing to provide a high resolution of the state variables. A total of 25000 quadrilateral elements are used, as a finer mesh is not possible with the FEM software.

The workpiece material is modeled as rigid-viscoplastic, homogeneous, with a constitutive relation that obeys the J_2 flow theory of plasticity with isotropic hardening. The relevant material constants of Ti6Al4V are temperature dependent [13]. The cutting tool is defined by a zero rake angle (γ=0^o) and is assumed to be non deformable. It is generally acknowledged that in comparison with the large plastic deformation of the workpiece material, the tool elastic deflection can be neglected without loss of accuracy. Therefore, it is modeled as a rigid body and only thermal properties are defined. An unstructured mesh of 4-node quadrilateral elements is used on the tool for thermal calculations. Finally, a high-quality mesh at the tool tip region has been considered to eliminate the need for remeshing during the course of the simulation.

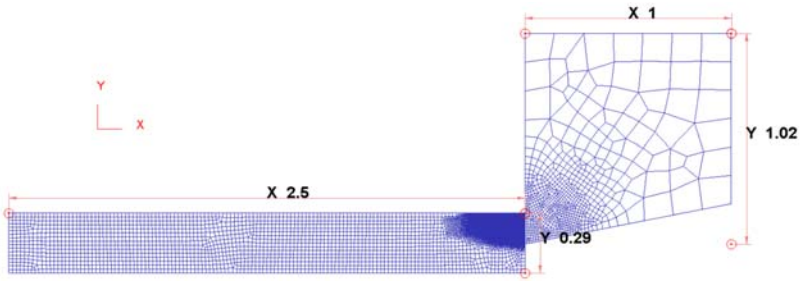

Figure 1. The configuration of the orthogonal cutting problem.

4.2 Adiabatic shear band propagation

A sequence of results, which describe the evolution of the adiabatic shear band, are displayed in Figure 2. The cutting conditions are: cutting speed v=200 m/min, feed=0.15 mm/rev and rake angle γ=0^o. The maximum scale of temperature, equivalent strain and equivalent stress have been set to a value of 600 ^{o}C, 3.7 and 1320 MPa, respectively. As revealed from the simulation the mechanism proceeds with the following order:

At an initial stage (a), an ASB commences in front of the tool tip and propagates almost straight along the primary shear zone. Shearing occurs rapidly enough so that heat generated from plastic work conversion cannot be quickly dissipated from the band (see stages b and c). Inside the ASB the resistance to continued loading becomes lower than the surrounding material and strain tends to concentrate further. The additional deformation generates more heat causing the material inside the band to become even softer. Essentially, temperature rise enforces strain localization and vice versa, further amplifying the non uniformity in strain, and hence, the ASB becomes the weakest zone in the cutting region. A drop of the equivalent stress (von Mises) inside the ASB can be seen in stages (b) and (c). This mechanism of strain localization destabilizes the homogeneous plastic deformation and is responsible for the formation of chip segments at high cutting speeds. While the tool moves forward (beyond stage c), the ASB gradually curves upwards. Opposite to continuous chip formation in which shear takes place along the primary shear zone and remains fixed in space, when an ASB is formed, the strain continues to localize within this zone, so the ASB is carried away with the chip motion. Finally, a new ASB originates in front of the tool tip (stage f) following exactly the same mechanism as previously explained (see the similarity of the new formed ASB between the first (a) and the sixth (f) stage of Figure 3. The ASB can reform intermittently if the loading conditions are maintained. It is apparent that the temperature, the equivalent strain and the equivalent stress fields change periodically during the formation of a chip segment. This mechanism is leading to severe self induced vibrations during cutting and possible fatigue failure of the tool [28].

A high temperature gradient across the adiabatic shear band width can be clearly observed (Figure 2). The shear band is rapidly cooled due to heat conduction to the surrounding material when plastic deformation ceases. Simulation shows that the temperature distribution within a well formed adiabatic shear band is laminar. This result is consistent with the prevailing theoretical models in which the plastic flow within the adiabatic shear band has been assumed essentially laminar [29-31]. However, experimental observations revealed a highly

transient two-dimensional temperature field within a well developed adiabatic shear band [32], [33]. The authors seems to believe that this structure is highly non-uniform and possesses a transient, short range of periodicity in the direction of shear band growth like an array of intense 'hot spots', reminiscent of the well-known shear-induced hydrodynamic instabilities in fluids. Even though, the loading configuration of the aforementioned experiment, which is entirely different from the present case, is leading to the conclusion that there is a crucial need for deeper investigation of this issue in the future. A reasonable explanation of this laminar temperature flow inside the ASB is that the computational mesh size is not appropriate to capture the small scale structure inside the ASB.

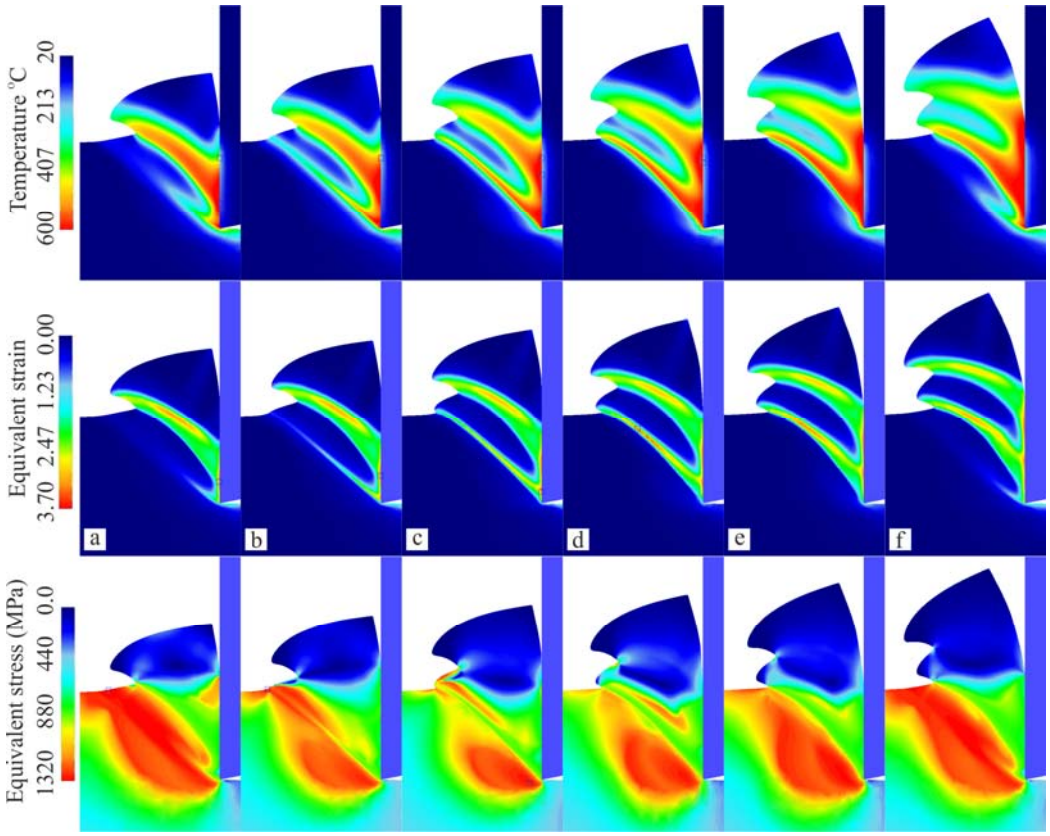

Figure 2. Temperature, equivalent strain, equivalent stress (von Mises) and damage contours at different stages (a-f) of the chip segment formation (v=200 m/min, feed=0.15 mm/rev, rake angle $\gamma=0^{o}$).

Furthermore, the thermal and mechanical behavior of the chip segmentation process at different cutting conditions is illustrated in Figure 3 and Figure 4. As revealed from Figure 3, a heat source that influences the ASB initiation and growth and becomes more significant at low cutting speeds is the friction at the interface of the deformed material and the cutting tool rake face. Thermal diffusion from this heat source acts as a stabilizing effect as it tends to equalize the temperature field and inhibits heat concentration into the ASB. At higher cutting speeds, the ASB heat source predominates (Figure 4). Although there is considerable research interest on the friction conditions, except for the cases mentioned just above, they do not significantly affect the initiation and evolution of ASB. A further simulation result refers to the chip compression ratio which decreases in relation to the cutting speed (Figures 3 and 4). In these figures it is observed that by increasing the cutting speed the segmentation frequency defined as the number of segments per chip length also increases. This is reasonable because by increasing the cutting speed the chip shearing and segmentation process is accelerated and consequently the shear band spacing is respectively affected. On the other hand by increasing the feed rate the segmentation frequency is reduced (Figures 2 and 4).

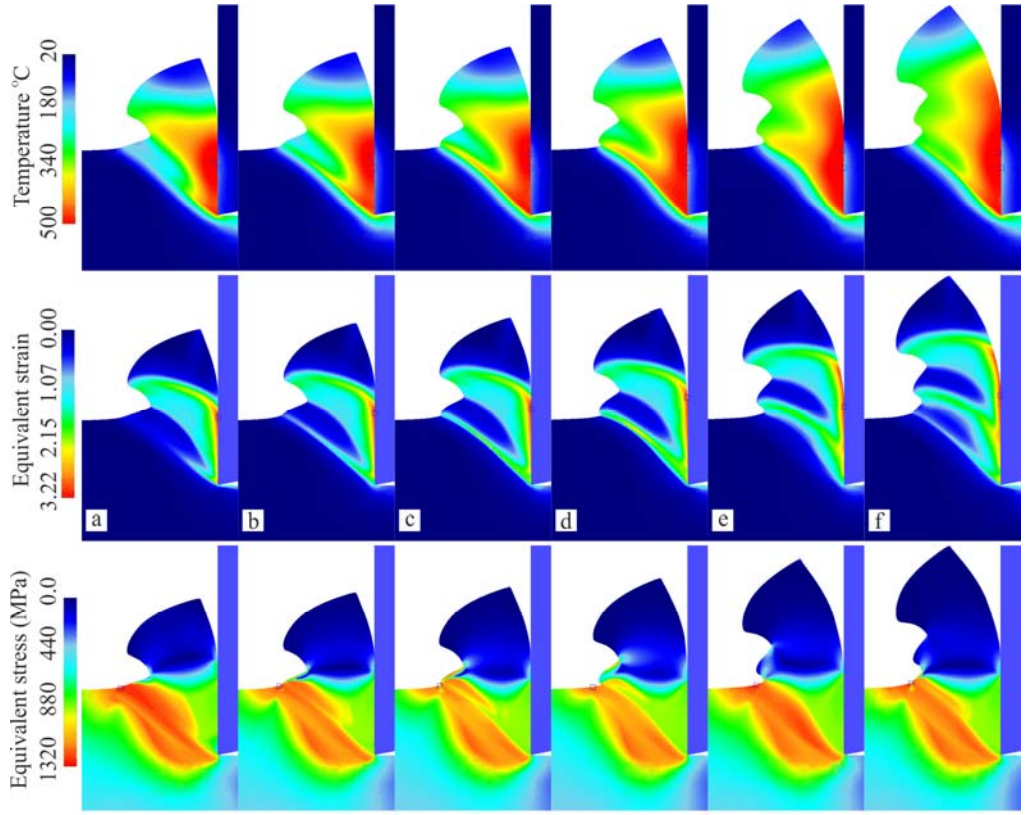

Figure 3. Temperature, equivalent strain, equivalent stress (von Mises) and damage contours at different stages (a-f) of the chip segment formation (v=50 m/s, feed=0.15 mm/rev, rake angle γ=0º).

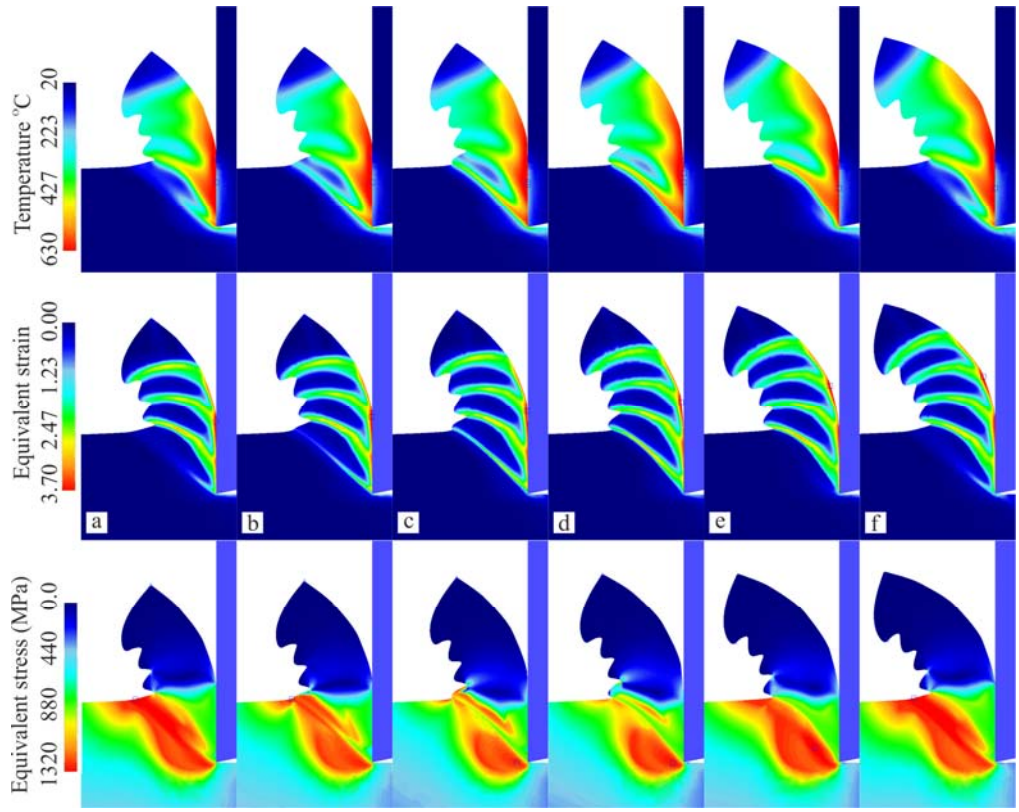

Figure 4. Temperature, equivalent strain, equivalent stress (von Mises) and damage contours at different stages (a-f) of the chip segment formation (v=200 m/s, feed=0.10 mm/rev, rake angle γ=0º).

5 DAMAGE COMPUTATION INSIDE ADIABATIC SHEAR BANDS

Ductile fracture has been widely studied as a process of void nucleation, growth and subsequent coalescence. There is experimental evidence that ductile fracture is also evident inside the ASB. According to experimental data (e.g., Marchand and Duffy, 1988), onset of the ductile failure via shearbanding occurs in a sudden, drastic way [34]. The same studies show that immediately following the onset of the ductile failure, the stress at the material point drops almost vertically to about a quarter of its peak value.

An excellent discussion on the necessity of a ductile failure criterion was given by Schoenfeld and Wright (2003), who identified the need for the introduction of what they call a 'shear damage' in order to model the stress collapse state inside an ASB, as well as the need for a ductile failure criterion in order to determine the right timing at which it should occur [35]. Such a criterion, if properly designed, could also shed some light on the physics of adiabatic shearbanding, as well as help to predict the susceptibility of different materials to this type of failure.

Sergey et al. (2007) postulated a physical criterion based on the hypothesis that material inside the shear band region undergoes a dynamic recrystallization process during deformation under high temperature and high strain-rate conditions [36]. They conducted large scale meshfree simulations to validate the proposed criterion by examining the formation, propagation, and post-bifurcation behaviors of ASBs in two materials, 4340 steel and OFHC copper.

Metallurgical examination of the adiabatic shear bands and the cracking present in the localized zones in Ti6Al4V samples deformed at low, medium and high deformation speeds showed that the hardness of these zones was not significantly higher than that of the surrounding metal and that the crack morphology was also consistent with that of ductile fracture [37, 38].

Considering the history of stress and strain at plastic deformation of metals, Cockcroft and Latham [39, 40] postulated that it is the principal tensile stress, rather than the generalized stress, which is important in fracture initiation. They proposed a damage criterion based on the strain energy density where the magnitude of the maximum principal stress component over the plastic strain path is taken into account, namely:

$$D_{cr} = \int_0^{\bar{\varepsilon}_f} \frac{\sigma_1}{\bar{\sigma}} d\bar{\varepsilon} \tag{3}$$

where $\bar{\varepsilon}_f$ is the total equivalent strain to failure, σ_1 is the maximum principal stress, $\bar{\sigma}$ and $\bar{\varepsilon}$ are the effective stress and strain, respectively, and D_{cr} is the maximum damage value, i.e. the critical damage value (CDV) of fracture. This criterion does not take into account the influenceof hydrostatic stress explicitly on fracture.The critical damage value D_{cr} depends on the same material parameters that forming limits are dependent on. Material properties such as chemical composition, microstructure, grain form, grain size, surface conditions, non-metallic inclusion content and homogeneity whilst having a small effect on the strength and the hardness, have a significant effect on the CDV. For homogeneous materials D_{cr} can be considered as material constant during given plastic deformation conditions (i.e temperature, rate of deformation, state of stress and deformation history) and it can be comprehended by analogy to the plasticity constant according to the Tresca and Misses [41]. Therefore, the dependence of the CDV on the temperature and strain rate must be carefully considered in ASB FEM simulations.

Rewriting equation (3) gives the integral I (in this case with a dimensionless critical value for fracture to occur):

$$I = \frac{1}{D_{cr}} \int_0^{\bar{\varepsilon}_f} \frac{\sigma_1}{\bar{\sigma}} d\bar{\varepsilon} \tag{4}$$

In FEM computation the integral (4) is calculated for each element at the integration points (Gauss points) at each deformation step, and the condition for fracture is satisfied when the integral I amounts to unity. Then the stiffness of the element is reduced to zero. The mechanical and thermal behavior during the formation of a chip segment when the Cockcroft & Latham ductile fracture criterion is implemented into the FEM code is illustrated in Figure 5. In the present simulation the dimensionless value for the CDV is set to 0.8 (see equation 4). The cutting speed is set to v=200 m/min and the feed equal to 0.1 mm/rev. In this case, two different mechanisms of catastrophic shear may occur simultaneously; thermoplastic shear and ductile fracture. The maximum scale of temperature, equivalent strain, equivalent stress, and damage contours has been set to values of 660ºC, 6.0, 1320 MPa, and 7.5, respectively. The color contour depicted on the surface of the workpiece is used so that one may compare the initial stage of shear band growth with the final stage of crack growth. The mechanism of chip segment formation proceeds as explained below.

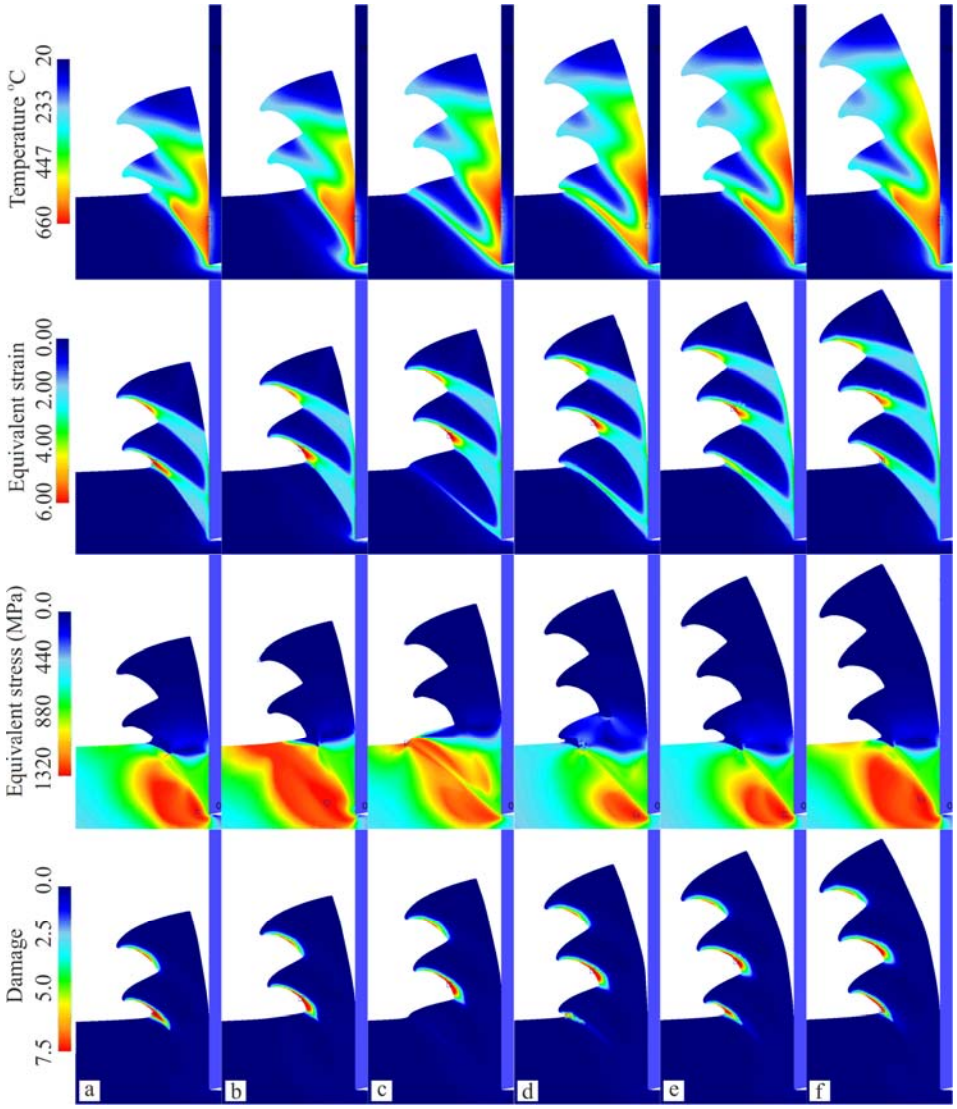

Figure 5. Temperature, equivalent strain, equivalent stress (von Mises) and damage contours at different stages (a-f) of the chip segment formation
(v=200 m/s, feed=0.10 mm/rev, rake angle γ=0°, normalized Cockroft& Latham CDV=0.8)

At an initial stage (a-b), the ASB initiates in front of the tool tip and propagates straight along the primary shear zone. Inside the ASB the material resistance to loading becomes lower than the surrounding material, since the heat generated from the plastic work cannot be quickly dissipated away from the band and strain tends to concentrate further. Note that the temperature and strain localization within the band can be clearly observed in all stages of the chip segmentation process (a-f). The stress begins to drop rapidly (c) and a rapid increase in temperature appears with a rate approximately of 17°C\μs. At stage (d) the stress collapses at the region near the free surface of the chip since the CDV is reached. It has to be remarked, that for elements which exceed the CDV value, a continuum damage softening is applied. Specifically, for an element that is exceeding D_{cr}, the calculated flow stress value used for the element stiffness equation is reduced to a specified percentage level (in the present simulations to 0.01% of the flow stress). The sudden drop of the equivalent von Mises stress at the region near the free surface indicates the initiation of cracks. One may see that there is a non-zero stress inside the downward part of ASB, whereas in the upward part of the strip the equivalent stress is zero, which indicates the separation of the specimen. This finding is in complete agreement with the mechanism proposed by Shaw and Vyas [42] explaining the segmented chip formation as a gross shear fracture extending from the free surface of the chip toward the tool tip. Additionally, in experiments conducted by various research groups (e.g. Affouard et al., 1984; Giovanola, 1988a,b), it has been observed that cracks follow the path weakened by the growing shear band, whose origin has been attributed to either brittle fracture, or damage induced microvoid growth and coalescence [43-45]. In our computations we observe a pattern of interface crack between the shear band and the

free surface. An interesting comparison of the CDV influence on the ASB propagation shows that as CDV decrease, the damage zone inside the shear band is progressively extended.From this stage and beyond, ductile fracture is the predominant mechanism of the chip segment formation, while the ASB is inevitably arrested at the lower boundary of the stress collapse region, as illustrated in the temperature and stress fields (see stages d-f). Thus it can be revealed that catastrophic shear occurs due to the synergistic effects of ductile fracture near the chip free surface. The ASB formation extends from the tool tip towards the lower end of the fracture zone. Consequently, as the tool moves further (stages e-f), the temperature increases more inside the ASB, while the heat diffuses to the adjacent material. Note also that the equivalent strain localization in the crack zone is an artifact of the simulation since a continuum damage softening is applied as previously explained. The maximum strain inside the band is about 3.8. In the investigated case, further cracks are not initiated within the ASB. At a final stage (f) a new ASB originates in front of the tool tip following exactly the same mechanism as previously mentioned. The above mechanism occurs intermittently if the loading conditions are maintained. It can be clearly seen that the temperature, the equivalent strain and the equivalent stress change periodically according to the chip segment formation.

7 CONCLUSIONS

The presented FEM modeling and simulation of Ti6AL4V orthogonal machining describes satisfactorily the chip segmentation process and the development of adiabatic shear bands. Both shear instability and/or fracture mechanics inside adiabatic shear zone at high strain rates and temperatures are considered.The results give interesting insight into the chip formation mechanism and the chip flow. The model serves as useful tool in studying the influence of the cutting conditionssuch as the cutting speed and tool federate on the machining process of titanium alloys.

8 ACKNOWLEDGEMENTS

This research has been co-financed by the European Union (European Social Fund–ESF) and Greek national funds through the Operational Program "Education and Lifelong Learning" of the National Strategic Reference Framework (NSRF)-Research Funding Program: ARCHIMEDES III investing in knowledge society through the European Social Fund.

REFERENCES

[1] Zener, C., Hollomon, J. H. (1944), “Effect of strain rate upon plastic flow of steel,”*J. Appl. Phys*. Vol. 15, pp. 22–32.
[2] Recht, R. F. (1964), “Catastrophic Thermoplastic Shear,”*Trans. ASME*, Vol. 31, pp. 189-193.
[3] Wright, T.W. (2002), The physics and mathematics of adiabatic shear bands, *Cambridge monographs on mechanics*.
[4] Shaw, M. C., Vyas, A. (1993), “Chip Formation in the Machining of Hardened Steel,”*Annals of the CIRP*, Vol. 42/1, pp. 29-33.
[5] Komanduri, R., Turkovivich, B.F. (1981), “New observations on the mechanism of chip formation when machining titanium alloys,”*Wear*, Vol. 69, pp. 179-188.
[6] Nakayama, K., Arai, M., Kanda, T. (1988), Machining characteristics of hard materials, *Annals of the CIRP*, Vol. 37 (1), pp. 89–9.
[7] Nakayama, K. (1974), “The formation of saw tooth chips,” *Proceedings of the International Conference on Production Engineering*, Tokyo, pp. 572–577.
[8] Vyas, A., Shaw, M. C. (1999), “Mechanics of saw-tooth chip formation in metal cutting,”*J. Manuf. Sci. Eng*., Vol. 121, pp. 163-172.
[9] Komanduri R. (1982), “Some clarifications on the mechanics of chip formation when machining titanium alloys,”*Wear*, Vol. 76, pp. 15-34.
[10] Rogers, H.C. (1979), “Adiabatic plastic deformation,”*Annual Rev. of Mat. Science*, Vol. 9, pp. 283–311.
[11] Zienkiewicz, O.C., Godbole, P.O. (1974), “Flow of plastic and visco-plastic solids with special reference to extrusion and forming processes,”*Int. J. Num. Meth. in Eng*., Vol. 8, pp. 3-16.
[12] Kobayashi, S., Oh, S.I., Altan, T. (1989), Metal Forming and the Finite-Element Method, Oxford University Press.
[13] DEFORM-2D Scientific Forming Technologies Corporation.
[14] Ortiz, M., Leroy Y., Needleman, A. (1987), “A finite element method for localized failure analysis, *Comput. Method Appl. Mech. Engrg*.,” Vol. 61, pp.189-214.
[15] Fish, J., Belytschko, T., (1988), “Elements with embedded localization zones for large deformation problems,”*Comput. & Structures*, Vol. 30, pp. 247.
[16] Marusich, T.D., Ortiz, M. (1995), “Modeling and Simulation of High-Speed Machining,”*International Journal for Numerical Methods in Engineering*, Vol. 38/21, pp. 3675–3694.

[17] El-Magd, E., Treppmann, C. (1999), "Simulation of Chip Root Formation at High Cutting Rates by Means of Split-Hopkinson Bar Test", *Materialpruefung, German Journal: Mat. Testing*, Vol. 41/11, pp. 457–460.
[18] Treppmann, C. (2001), "Flieverhalten metallischer Werkstoffe bei Hochgeschwindigkeitsbeanspruchung", Dissertation, RWTH Aachen, Germany.
[19] Baker, M. (2003), "The influence of plastic properties on chip formation", *Computational Materials Science*, Vol. 28, pp. 556–562.
[20] Taylor, G. I., Quinney, H. (1934), "The latent energy remaining in a metal after cold working", *Proc. R. Soc. Lond*. A, Vol. 143, pp. 307-326.
[21] Mason, J.J., Rosakis, A.J., Ravichandran, G. (1994), "On the strain and strain rate dependence of the fraction of plastic work converted to heat: an experimental study using high speed infrared detectors and the Kolsky bar", *Mech. Mat*., Vol.17, pp.135-145.
[22] Kapoor, R., Nemat-Nasser, S., (1998) "Determination of temperature rise during high strain rate deformation", *Mech. Mat*., Vol. 27, pp.1-12.
[23] Nemat-Nasser, S., Guo, W.G., Nesterenko, V.F., Indrakanti, S.S., Gu, Y.B. (2001), "Dynamic response of conventional and hot isostatically pressed Ti6Al4V alloys: experiments and modeling", *Mech. Mater*., Vol. 33, (8), pp. 425-439.
[24] Duncan, A. S., Macdougall, P., Maudlin, J., (2000), "The proportion of plastic work converted to heat in Ti-6Al-4V: MTS model prediction and experimental data", Explomet, June 19-23, Albuquerque, NM.
[25] Rosakis, P., Rosakis, A. J., Ravichandran, G., Hodowany, J., (2000), "A thermodynamic internal variable model for the partition of plastic work into heat and stored energy in metals", *J. Mech. Phys. Solids*, Vol. 48 (3), pp. 581-607.
[26] Childs, T.H., Dirikolu, M.H., Sammons, M.D.S., Maekawa, K., Kitagawa, T. (1997), "Experiments on and Finite Element Modeling of Turning Free-Cutting Steels at Cutting Speeds up to 250 m/min", *Proceedings of 1st French and German Conference on High-speed Machining*, pp. 325–331.
[27] Wright, P.K., Horne, J.G., Tabor, D. (1979), "Boundary Conditions at the Chip-Tool Interface in Machining: Comparisons Between Seizure and Sliding Friction,"*Wear*, Vol. 54, pp. 371–390.
[28] Albrecht P. (1962), "Self induced vibrations in metal cutting,"*J. Eng. Ind.*, Vol. 84, pp 415.
[29] Wright T.W. Ravichandran G. (1997), "Canonical aspects of adiabatic shear bands,"*International Journal of Plasticity*, 13 (4), pp. 309–325.
[30] Molinari A. Leroy Y.M. (1990), "Existence and Stability of Stationary Shear Bands With Mixed-Boundary Conditions,"*C. R. Acad. Sci.*, Série II, V. 310 (8), pp. 1017-1023.
[31] Gioia G. Ortiz M. (1996), "The two-dimensional structure of dynamic boundary layers and shear bands in thermoviscoplastic solids,"*J. Mech. Phys. Solids*, Vol. 44 (2), pp. 251-292.
[32] Guduru P.R. Ravichandran G. Rosakis A.J. (2001), "Observations of transient temperature vortical microstructures in solids during adiabatic shear banding,"*Physical Review E*, Vol. 64(3), pp. 036128.
[33] Guduru P.R. Rosakis A.J. Ravichandran G. (2001), "Dynamic shear bands: an investigation using high speed optical and infrared diagnostics,"*Mechanics of Materials*, Vol. 33, pp. 371–402.
[34] Marchand, A., Duffy, J.(1988), "An experimental study of the formation process of adiabatic shear bands in a structural steel,"*J. Mech. Phys. Solids* 36 (3), pp. 251-283.
[35] Schoenfeld, S.E., Wright, T.W.(2003), "A failure criterion based on material instability,"*International Journal of Solids and Structures*, 40, pp. 3021-3037.
[36] Sergey N. Medyanika, Wing KamLiua, Shaofan Li (2007), "On criteria for dynamic adiabatic shear band propagation,"*Journal of the Mechanics and Physics of Solids*, Vol. 55, pp. 1439–1461.
[37] Lee, D. (1985), "The effect of cutting sped on chip formation under orthogonal machining,"*J. Eng. Ind*., *Trans. ASME*, Vol.107 (1), pp. 55-63.
[38] Kailas, S.V., Prasad, Y.V.R.K., Biswas, S.K. (1994), "Flow instabilities and fracture in Ti-6Al-4V deformed in compression at 298-673 K,"*Metall. Mater. Trans*. A, Vol. 25A, pp. 2173-2179.
[39] M.G. Cockcroft (1968), *Ductility*, American Society for Metals, Metals Park, Ohio, pp. 199-226.
[40] M.G. Cockcroft and D.J. Latham (1968), "Ductility and workability of materials,"*Journal of the Institute of Metals*, Vol. 96, pp. 33-39.
[41] AvitzurB. (1968), Metal forming process and analysis, Mc GrawHill Book Company New York.
[42] Shaw, M. C., Vyas, A. (1993),"Chip Formation in the Machining of Hardened Steel,"*Annals of the CIRP*, Vol. 42/1, pp. 29-33.
[43] Affouard, J.L., Dormeval, R., Stelly, M., Ansart, J.P.(1984),"Adiabatic shear bands in metals and alloys under dynamic compressive conditions. In: Harding, J. (Ed.),"*Proceedings of the Third Conference on the Mechanical Properties at High Rates of Strain*, Oxford, UK, pp. 533–540.
[44] Giovanola, J.(1988a),"Adiabatic shear banding under pure shear loading. 1. Direct observation of strain localization and energy measurements,"*Mechanics of Materials*, Vol. 7, pp. 59–71.
[45] Giovanola, J.(1988b),"Adiabatic shear banding under pure shear loading. 2. Fractographic and metallographic observations, "*Mechanics of Materials*, Vol. 7,pp. 72–87.